A Systematic Research on the Synthesis, Structures, and Application in Photocatalysis of Cluster-Based Coordination Complexes

ARTICLE *in* CRYSTAL GROWTH & DESIGN · JANUARY 2014

Impact Factor: 4.89 · DOI: 10.1021/cg401601d

7 AUTHORS, INCLUDING:

Jie Ding
Zhengzhou University
25 PUBLICATIONS **258** CITATIONS

CRYSTAL GROWTH & DESIGN

Article

pubs.acs.org/crystal

A Systematic Research on the Synthesis, Structures, and Application in Photocatalysis of Cluster-Based Coordination Complexes

Wei Meng,[†] Zhouqing Xu,[†,‡] Jie Ding,*[,†] Dongqing Wu,[†] Xiao Han,[†] Hongwei Hou,*[,†] and Yaoting Fan[†]

[†]The College of Chemistry and Molecular Engineering, Zhengzhou University, Zhengzhou, 450052, People's Republic of China

[‡]Department of Physics and Chemistry, Henan Polytechnic University, Jiaozuo, 454000, People's Republic of China

Supporting Information

ABSTRACT: To search for effective photocatalysts in the field of cluster-based coordination complexes, we synthesized $\{[Cd_2(dcpp)(beb)_2\ (H_2O)]\cdot H_2O\}_n$ (**1**), $[Cd_2(dcpp)(bmb)(H_2O)_2]_n$ (**2**), $\{[Cd_2(dcpp)(2,2'\text{-bipy})(H_2O)_2]\cdot 2H_2O\}_n$ (**3**), and $\{[Cd_2(dcpp)(4,4'\text{-bipy})_{0.5}(H_2O)_3]\cdot H_2O\}_n$ (**4**) by utilizing a butterfly-shaped multidentate carboxylic acid (4,5-di(4′-carboxylphenyl)phthalic acid) (H_4dcpp)) and N-donor ligands (1,4-bis(2-ethylbenzimidazol-1-ylmethyl) benzene (beb), 1,4-bis(2-methylbenzimidazol-1-ylmethyl) benzene (bmb), 2,2′-bipyridine (2,2′-bipy), 4,4′-bipyridine (4,4′-bipy)). Complexes **1**−**4** are constructed based on different SBUs. Complexes **1** and **2** possess three-dimensional (3D) pillar-layered frameworks based on noncluster-type SBUs and dinuclear Cd_2 clusters units, respectively. Complex **3** is a 3D porous structure building on Cd_4 clusters SBUs. Complex **4** is constructed from rare infinite botryoid-like Cd cluster chains and exhibits a 3D complicated framework. The research on optical energy gaps of complexes **1**−**4** indicates that these complexes are potential semiconductive materials. Moreover, complexes **1**−**4** are applied to catalyze the reaction of photocatalytic degradation of methylene orange (MO) under high-pressure mercury lamp irradiation. Excitingly, they exhibit good photocatalytic properties in the presence of H_2O_2, and the degradation rates for **1**−**4** increase from 43% (without photocatalyst) to 97, 78, 85, and 67%, respectively, after 100 min of irradiation. The photoluminescent properties of complexes **1**−**4** were also studied.

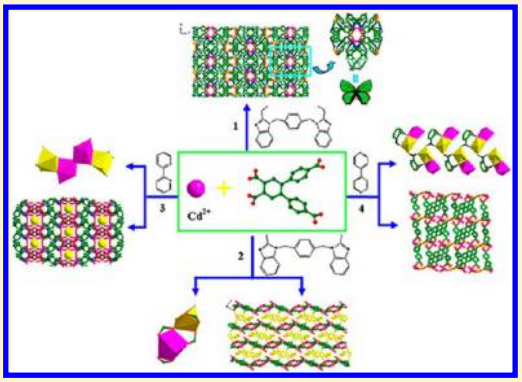

INTRODUCTION

Recently, humanity is faced with tremendous environmental problems related to the remediation of contaminated groundwater, hazardous wastes, and the control of toxic air contaminants. In particular, the problem about the treatment of wastewater has emerged as a high national and international priority. The discharge of harmful dyes into water not only pollutes water bodies but also affects aquatic life.[1] There have been considerable efforts in treating wastewater based on adsorption and separation,[2] chemical treatment,[3] and photocatalytic methods.[4] Among these, photocatalysis offers a convenient and recyclable approach and has been applied in ecologically eliminating organic dyes and other noxious contaminants. Therefore, the investigation of inexpensive, stable, and efficient materials with improved photocatalytic properties is extremely urgent.

Though many materials as photocatalysts have been investigated for decomposing organic dyes, the exploration of cluster-based coordination complexes as effective photocatalysts is relatively rare.[5] To search for a more effective photocatalyst, we have been interested in the synthesis of materials in the field of cluster-based coordination complexes. As we know, the construction of secondary building units (SBUs) is becoming an effective synthetic method to manufacture cluster-based coordination complexes.[6] SBUs, as carriers of structure and function, take the responsibility for diverse performances of the complexes.[7−11] We believe that the rational design and synthesis of complexes with diverse SBUs can provide potential application in photocatalytic decomposition of organic dyes. However, the regulation and construction of SBUs by proper organic ligands and metal nodes still remains a long-term work, and a systematic study is indispensable to enriching and developing the field.

On the basis of the above considerations, by employing a novel and less-explored butterfly-shaped ligand H_4dcpp,[12] and a series of auxiliary ligands beb, bmb, 2,2′-bipy, and 4,4′-bipy (Scheme S1, Supporting Information), we herein successfully synthesized four coordination complexes with different SBUs, namely, $\{[Cd_2(dcpp)(beb)_2\ (H_2O)]\cdot H_2O\}_n$ (**1**), $[Cd_2(dcpp)(bmb)(H_2O)_2]_n$ (**2**), $\{[Cd_2(dcpp)(2,2'\text{-bipy})(H_2O)_2]\cdot 2H_2O\}_n$ (**3**), and $\{[Cd_2(dcpp)(4,4'\text{-bipy})_{0.5}(H_2O)_3]\cdot H_2O\}_n$ (**4**). We also explored the optical energy gap and the emission spectra of the four complexes. The reflectance spectra show that there exist the optical band gap and semiconductive behaviors in complexes **1**−**4**, and the complexes can be employed as possible semiconductive materials. Moreover, complexes **1**−**4**

Received: October 28, 2013
Revised: January 2, 2014
Published: January 7, 2014

   dx.doi.org/10.1021/cg401601d | *Cryst. Growth Des.* 2014, 14, 730−738

Table 1. Crystallographic Data of 1−4[a,b]

complex	1	2	3	4
formula	$C_{74}H_{66}N_8O_{10}Cd_2$	$C_{46}H_{36}N_4O_{10}Cd_2$	$C_{32}H_{26}N_2O_{12}Cd_2$	$C_{27}H_{22}NO_{12}Cd_2$
formula mass	1452.15	1029.59	855.35	777.26
crystal system	orthorhombic	triclinic	monoclinic	monoclinic
space group	*pccn*	$P\bar{1}$	*C*2/*c*	*P*2(1)/*c*
wavelength [Å]	0.71075	0.71073	0.71073	0.71073
temp [K]	113(2)	293(2)	293(2)	293(2)
a (Å)	45.787(15)	10.933(2)	29.426(6)	17.001(3)
b (Å)	16.599(5)	14.321(3)	9.1549(18)	8.5304(17)
c (Å)	15.858(6)	14.435(3)	27.559(6)	23.469(8)
α (deg)	90.00	67.19(3)	90.00	90.00
β (deg)	90	14.435(3)	115.50(3)	127.642(19)
γ (deg)	90.00	71.99(3)	90	90.00
V (Å^3)	13572(8)	1981.2(7)	6701(2)	2695.1(12)
Z	8	2	8	4
D_{calcd} (g·cm^{-3})	1.421	1.726	1.696	1.916
F(000)	5936	1032	3392	1532
μ (mm^{-1})	0.692	1.142	0.779	1.647
GOF	1.146	1.122	1.196	1.139
R_1 ($I > 2\sigma(I)$)	0.1103	0.0533	0.0692	0.0671
wR_2 ($I > 2\sigma(I)$)	0.2665	0.1246	0.1695	0.1708

[a] $R_1 = \sum||F_o| - |F_c||/\sum|F_o|$. [b] $wR_2 = [\sum w(F_o^2 - F_c^2)^2/\sum w(F_o^2)^2]^{1/2}$.

exhibit good photocatalysis activities for photodegradation of MO under high-pressure mercury lamp irradiation.

EXPERIMENTAL SECTION

Materials and Methods. The lab supplies were purchased in a commercial way. The FLASH EA 1112 Series was used to determine the contents of C, H, and N. The Bruker Tensor 27 spectrophotometer recorded the IR spectra (KBr disk). The NETZSCH STA 449C thermogravimetric analyzer was used to investigate the thermal stability of all the samples in flowing air with a 10 °C/min heating rate between 25 and 800 °C. The X'Pert X-ray PANalytical diffractometer with the radiation of Cu Kα_1 was employed to measure the PXRD data. The Hitachi F-4500 fluorescence spectrophotometer measured the emission spectra of the solid samples with the pass width of 2.5 nm. The Cary Series UV−vis-NIR spectrophotometer containing an integrating sphere of 110 nm in diameter recorded the UV−vis spectra of all the samples in the range of 200−800 nm. $BaSO_4$ is considered as a scale of 100% reflectance.

Synthesis of {[Cd_2(dcpp)(beb)$_2$(H_2O)]·H_2O}$_n$ (1). H_4dcpp (20.3 mg, 0.05 mmol), $Cd(OAc)_2{\cdot}2H_2O$ (26.6 mg, 0.1 mmol), beb (19.7 mg, 0.05 mmol), and distilled H_2O (8 mL) were put into a Teflon-lined stainless steel container (25 mL). The mixture was heated at 140 °C for 4 days and cooled at 5 °C/h to room temperature. Then colorless prismatic crystals of **1** were collected with 72% yield (based on Cd). Anal. Calcd for $C_{74}H_{66}N_8O_{10}Cd_2$ (%): C, 61.20; H, 4.58; N, 7.72. Found: C, 60.95; H, 4.36; N, 7.85. IR (KBr, cm^{-1}): 3385(w), 3058(w), 2938(w), 1942(w), 1706(w), 1583(m), 1558(m), 1532(m), 1471(m), 1396(s), 1347(m), 1296(m), 1257(m), 1216(w), 1178(w), 1076(m), 1017(m), 965(w), 925(w), 853(s), 811(s), 787(m), 741(s), 716(s), 694 (w), 673(w).

Synthesis of [Cd_2(dcpp)(bmb)(H_2O)$_2$]$_n$ (2). **2** was collected with 54% yield (based on Cd) by replacing beb with bmb (18.3 mg, 0.05 mmol). Anal. Calcd for $C_{46}H_{36}N_4O_{10}Cd_2$ (%): C, 53.66; H, 3.52; N, 5.44. Found: C, 53.07; H, 3.50; N, 5.51. IR (KBr, cm^{-1}): 3056(w), 1582(w), 1558(w), 1526(m), 1475(m), 1455(m), 1340(s), 1347(m), 1291(m), 1230(w), 1160(w), 1106(w), 1015(m), 977(w), 951(w), 924(w), 857(m), 814 (m), 788(m), 736(s), 718(m), 694(w), 677(w).

Synthesis of{[Cd_2(dcpp)(2,2′-bipy)(H_2O)$_2$]·2H_2O}$_n$ (3). **3** was collected with 48% yield (based on Cd) by replacing bmb with 2,2′-bipy (7.8 mg, 0.05 mmol). Anal. Calcd for $C_{32}H_{26}N_2O_{12}Cd_2$ (%): C, 44.93; H, 3.06; N, 3.28. Found: C, 44.46; H, 3.06; N, 3.10. IR (KBr, cm^{-1}): 3390(w), 3041(w), 1940(w), 1577(m), 1533(m), 1489(w), 1439(w), 1387(s), 1337(w), 1181(w), 1158(m), 1103(m), 1062(w), 1018(m), 921(m), 869(m), 856(m), 811(m), 788(s), 765(s), 734(s), 716 (m), 683(w).

Synthesis of {[Cd_2(dcpp)(4,4′-bipy)$_{0.5}$(H_2O)$_3$]·H_2O}$_n$ (4). **4** was collected with 43% yield (based on Cd) by replacing bmb with 4,4′-bipy (7.8 mg, 0.05 mmol). Anal. Calcd for $C_{27}H_{22}NO_{12}Cd_2$ (%): C, 41.72; H, 2.85; N, 1.80. Found: C, 41.93; H, 2.66; N, 1.77. IR (KBr, cm^{-1}): 3081(w), 1607(w), 1581(w), 1530(s), 1385(s), 1346(s), 1287(w), 1223(m), 1175(m), 1141(w), 1094(m), 1063(m), 1026 (m), 982(w), 924(m), 855(m), 839(w), 812(m), 784(s), 721(s), 505(m), 686(w), 669(m).

Crystallography. Crystal data for complex **1**−**4** were determined by the Rigaku 007HF Saturn 724 CCD diffractometer at 113 K (**1**) or the Rigaku Saturn 724 CCD diffractometer at room temperature (**2**−**4**) with Mo Kα (λ = 0.71073 Å) radiation. After Lorentz and polarization corrections, all the data were obtained. The solution and refinement of the structures were performed with the SHELXL-97 crystallographic software package.[13] H atoms were located in the calculated positions and were refined by adopting a riding model. Crystallographic data as well as bond lengths and angles are displayed in Table 1 and Table S1 (Supporting Information), respectively.

Photocatalytic Measurement. A photocatalytic experiment in aqueous solution was carried out in a typical process. A 30 mg portion of photocatalyst and 2 mL of 30% H_2O_2 were added into the methyl orange aqueous solutions (120 mL, 11.11 mg/L). The mixture was stirred for half an hour in a dark environment to get a balance between adsorption and desorption. Then, with the radiation of a 500 W high-pressure Hg lamp, the solution was stirred constantly. Every 20 min, we took a 5 mL sample from the reaction system and the supernatant liquid obtained by centrifugation was used for the UV−visible analysis. The characteristic peak (λ = 465 nm) for methyl orange was employed to monitor the photocatalytic decomposition process.

RESULTS AND DISCUSSION

Crystal Structure of {[Cd_2(dcpp)(beb)$_2$(H_2O)]·H_2O}$_n$ (1). In complex **1**, the asymmetric unit contains two crystallographically independent Cd(II), one dcpp^{4-}, two beb, one coordinated H_2O, and one guest H_2O molecule. Cd1 is seven-coordinated and surrounded by four O atoms (O1, O2, O3A, and O4A) of two dcpp^{4-}, two N atoms (N1, N4) of two beb, and one O9 atom of one H_2O molecule. At Cd2, the

dx.doi.org/10.1021/cg401601d | Cryst. Growth Des. 2014, 14, 730−738

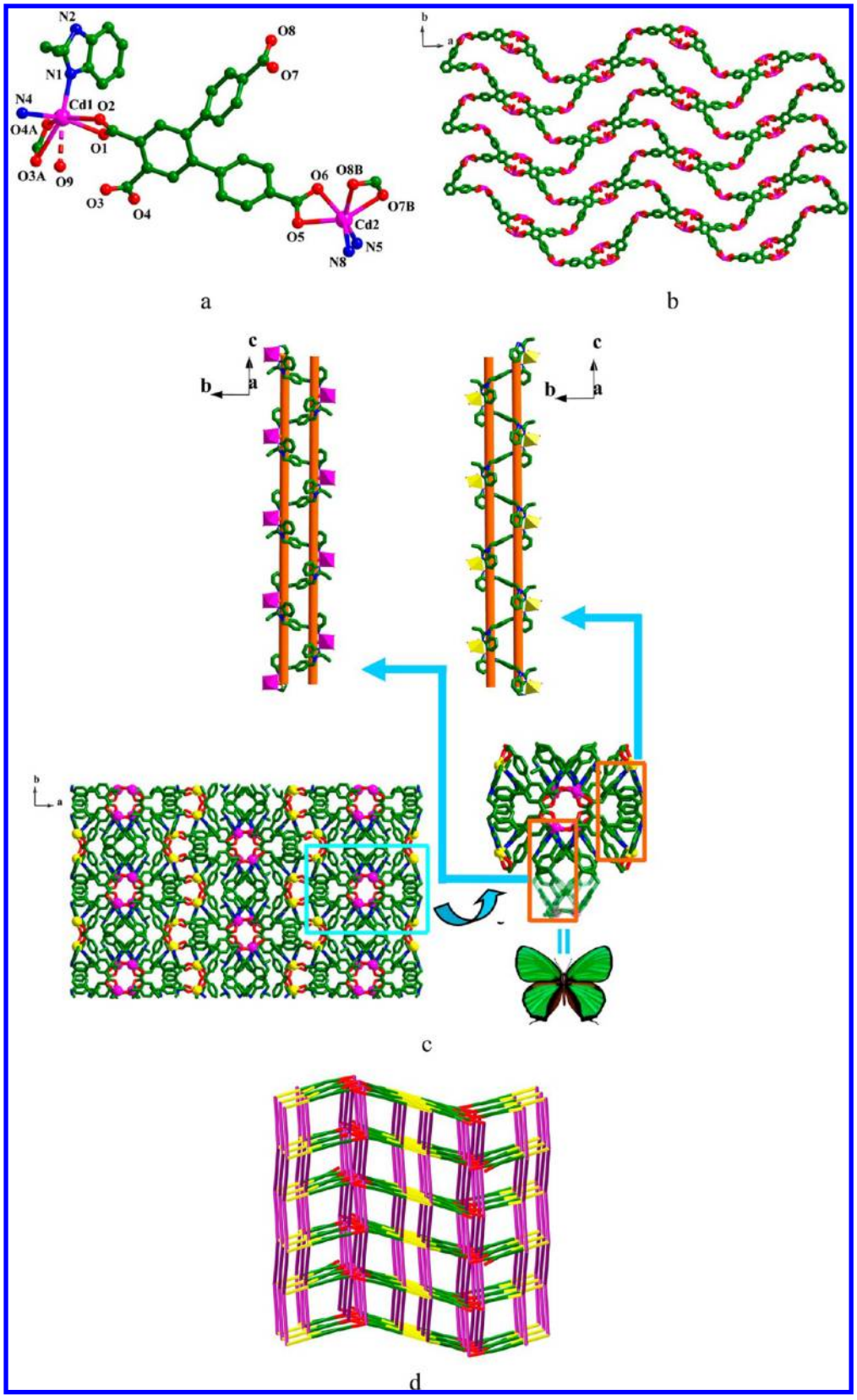

Figure 1. (a) Coordination environment around Cd^{II} in **1**. (b) The 2D wavelike layer constructed by $dcpp^{4-}$ and Cd^{II}. (c) The packing design sketch along the *c* axis: beautiful butterfly-like motifs arrange alternately (below) with two Cd2-N5 meso-helical chains as one pair of "wings", two half Cd1-N1 meso-helical chains as the "body", and two half Cd1-N1 helical as "antenna" (above). (d) The pillar-layered skeleton with $(6^4{\cdot}8^2)(4{\cdot}6^2{\cdot}8^3)_2$ topology.

coordination environment is a distorted octahedron with the equatorial plane occupied by three O atoms (O5, O7B, and O8B) and one N5 atom. The axial sites are occupied by one O6 atom and one N8 atom (Figure 1a). The distances of Cd1—

dx.doi.org/10.1021/cg401601d | *Cryst. Growth Des.* 2014, 14, 730−738

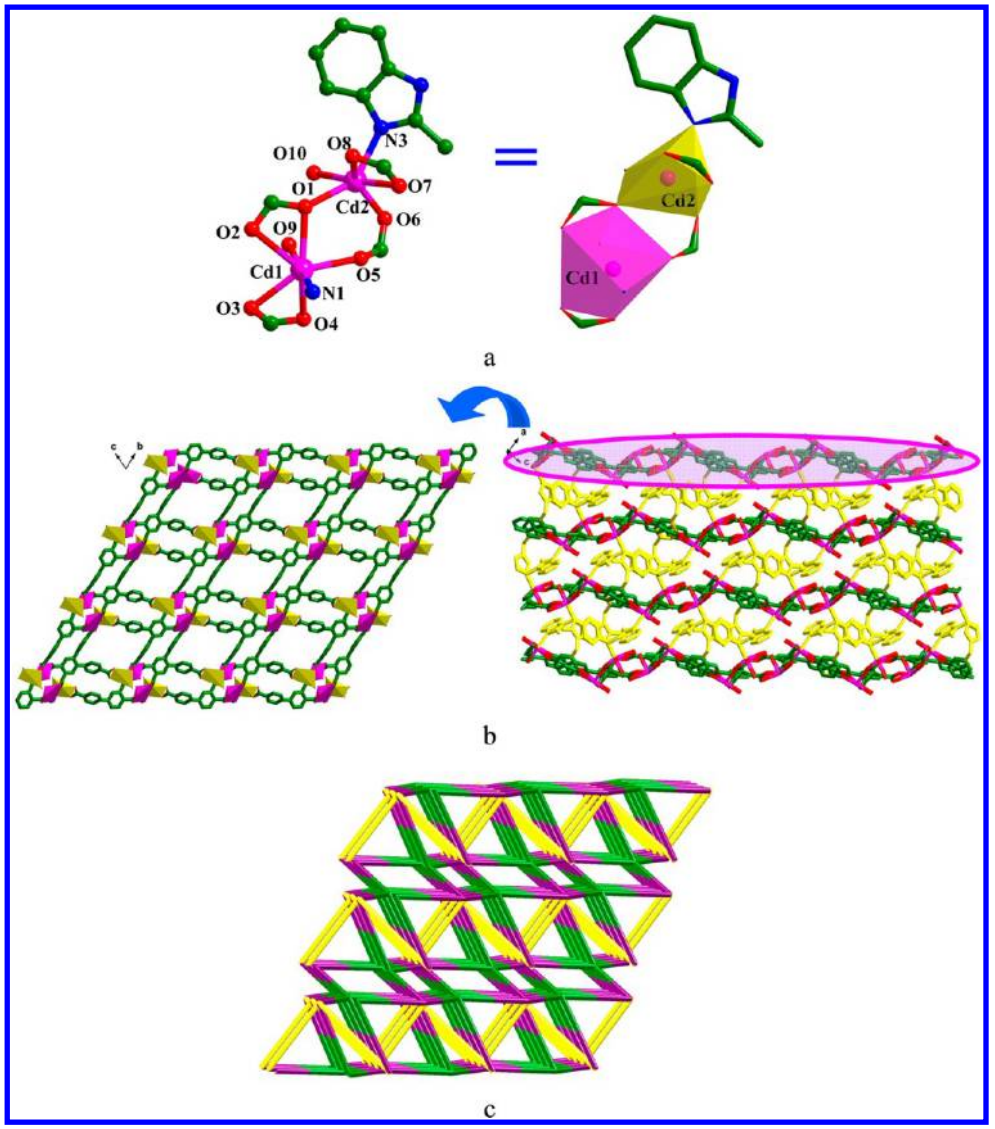

Figure 2. (a) Coordination environment around Cd^{II} in **2** (left) and the corner-shared dinuclear SBU (right). (b) The botryoid-like Cd cluster SBU. (c) The (4,6)-connected net with $(4^4{\cdot}5{\cdot}6^8{\cdot}7{\cdot}8)(4^2{\cdot}5{\cdot}6)$ topology.

O3A (2.760 Å) and Cd1−O9 (2.716 Å) are much longer than other Cd−O distances (Table S1, Supporting Information), indicating weak interactions between Cd1 and O3A, as well as Cd1 and O9. In complex **1**, four carboxylate groups of the $dcpp^{4-}$ adopt the (κ^2)-(κ^2)-(κ^2)-(κ^2)-μ_4 coordination mode (Scheme S2, Mode I, Supporting Information). The $dcpp^{4-}$ links Cd1 and Cd2 to manufacture a 2D wavelike layer (Figure 1b). Two independent beb all display an asymmetrical *cis*-conformation (Figure S1a, Supporting Information). The $N_{donor}{\cdots}N{-}C_{sp3}{\cdots}C_{sp3}$ torsion angles are 80.7° and 106.1°, respectively, for N1 containing beb (with $N_{donor}{\cdots}N_{donor}$ = 10.5301 Å and Cd1···Cd1 = 14.655 Å), and 63.4° and 101.8°, respectively, for N5 containing beb (with $N_{donor}{\cdots}N_{donor}$ = 11.067 Å and Cd2···Cd2 = 14.823 Å). Interestingly, along the *a* axis, the beb and Cd(II) produce two types of meso-helical chains with a pitch of 17.8580 Å, respectively: one consists of Cd1 and N1 containing beb, and another consists of Cd2 and N5 containing beb. The meso-helical chains pillar further the 2D layers to yield a 3D structure.

Another structural feature can be found in **1**. Viewing from the packing design sketch of **1** along the *c* axis (Figure 1c), beautiful butterfly-like motifs arranged alternately, with two Cd2-N5 meso-helical chains as "wings", two half of Cd1-N1 meso-helical chains as the "body", and two half of Cd1-N1 helical as "antenna". Topological analysis of **1** reveals that, if Cd1, Cd2, and the $dcpp^{4-}$ are viewed as 4-connected nodes, respectively, the 3D skeleton can be symbolized as a (4,4,4)-connected net with a point symbol $(6^4{\cdot}8^2)(4{\cdot}6^2{\cdot}8^3)_2$ (Figure 1d).

Crystal Structure of $[Cd_2(dcpp)(bmb)(H_2O)_2]_n$ (2). Complex **2** is also a pillar-layered skeleton. Cd1 is seven-coordinated with five O atoms (O1, O2, O3, O4, O5) of three $dcpp^{4-}$, one N1 atom of one bmb, and one O9 atom of one H_2O molecule. Cd2 locates in a distorted octahedral environment with the equatorial plane occupied by four O atoms (O6, O7, O8, O10) of two $dcpp^{4-}$, and the axial sites are occupied by one N3 atom of one bmb and one O1 atom of one $dcpp^{4-}$ (Figure 2a). The lengths of Cd−O/N agree well with those of the other Cd compound. The $dcpp^{4-}$ links six Cd(II) in the (κ^2)-$(\kappa^2$-$\mu_2)$-(κ^2)-$(\kappa^1$-$\kappa^1)$-μ_6 coordination fashion (Scheme S2, Mode II, Supporting Information). Cd1 are bridged to adjacent Cd2 by two carboxylate groups in $(\kappa^2$-$\mu_2)$ and $(\kappa^1$-$\kappa^1)$-μ_2

dx.doi.org/10.1021/cg401601d | *Cryst. Growth Des.* 2014, 14, 730−738

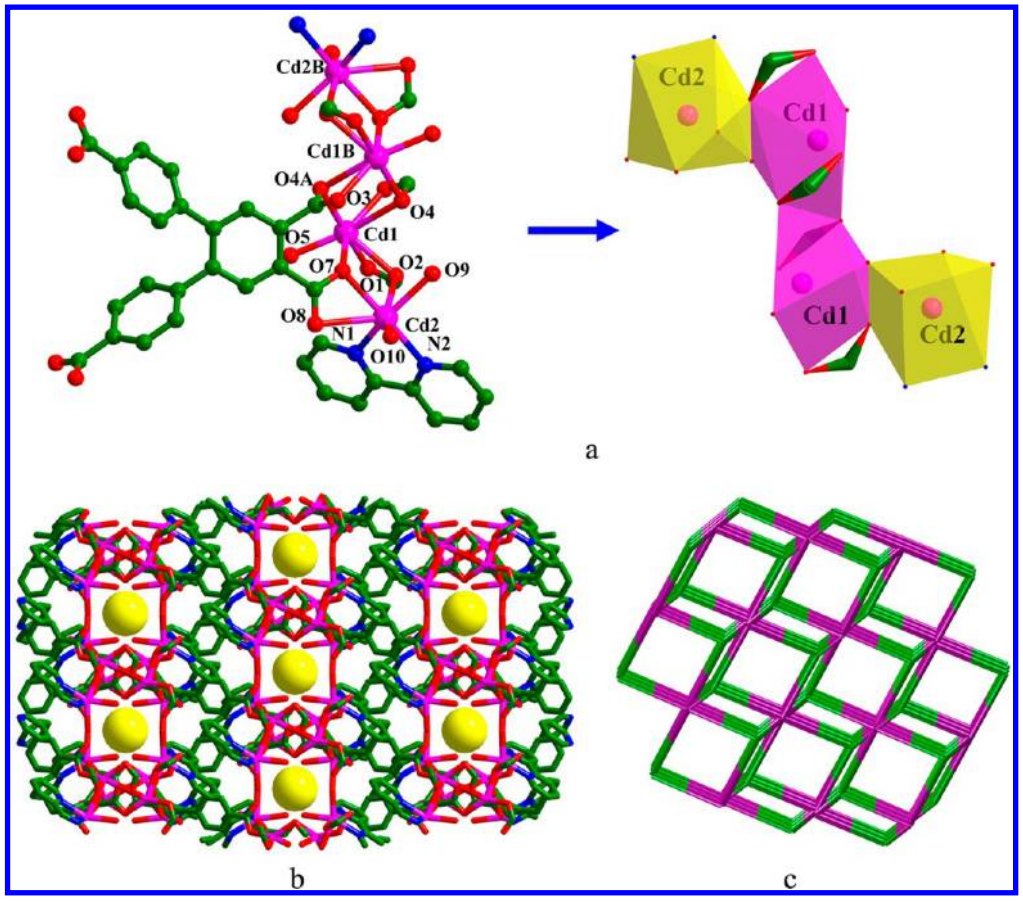

Figure 3. (a) Coordination environment around Cd^{II} in **3** (left) and the edge-shared tetranuclear SBU (right). (b) View of the pores and packing program of **3**. (c) The (3,6)-connected net with $(4^4{\cdot}6^2{\cdot}8^7{\cdot}10^2)(4^2{\cdot}6)$ topology.

modes, respectively, producing a corner-shared dinuclear unit where the Cd1···Cd2 separation is 3.9320 Å. Two neighboring binuclear units are linked by six $dcpp^{4-}$ to produce a 2D puckered layer (Figure 2b, left). These layers are then connected by two types of bmb into a 3D pillar-layered structure (Figure 2b, right). The bmb all adopt the *trans*-conformation (Figure S1b, Supporting Information), and the torsion angles of $N_{donor}{-}C_{sp3}{\cdots}C_{sp3}{-}N_{donor}$ are 180°. The torsion angles of $N_{donor}{\cdots}N{-}C_{sp3}{\cdots}C_{sp3}$ are 97.9° for N1 containing bmb (with $N_{donor}{\cdots}N_{donor}$ = 11.044 Å and Cd1···Cd1 = 14.829 Å) and 115.2° for N3 containing bmb (with $N_{donor}{\cdots}N_{donor}$ = 11.3442 Å and Cd2···Cd2 = 14.700 Å), respectively. Topological analysis of complex **2** is carried out. If the dinuclear cluster and the $dcpp^{4-}$ are considered as 6- and 4-connected nodes, respectively, then the skeleton of **2** could be simplified as a (4,6)-connected net with $(4^4{\cdot}5{\cdot}6^8{\cdot}7{\cdot}8)(4^2{\cdot}5{\cdot}6)$ topology (Figure 2c).

Crystal Structure of $\{[Cd_2(dcpp)(2,2'\text{-bipy})(H_2O)_2]\cdot 2H_2O\}_n$ (3). Complex **3** crystallizes in the monoclinic space group $C2/c$. The asymmetric unit includes two independent Cd(II), one $dcpp^{4-}$, one 2,2′-bipy, two coordinated H_2O molecules, and two guest H_2O molecules. Two Cd centers are seven-coordinated: Cd1 is surrounded by seven carboxylate O atoms (O1, O2, O3, O4, O4A, O5, and O7) of four $dcpp^{4-}$(Cd1−O = 2.157−2.629 Å), and Cd2 is surrounded by three carboxylate O atoms (O2, O7, and O8), two N atoms (N1 and N2) of one 2,2′-bipy, as well as two O atoms (O9 and O10) from two coordinated aqua ligands (Cd2−O/N = 2.254−2.458 Å) (Figure 3a). Cd1 and adjacent Cd2 are bound by two carboxylate groups to form a Cd_2 cluster in which the Cd1···Cd2 separation is 3.724 Å. Symmetrical expansion of the Cd_2 unit yields an unusual Cd_4 cluster as the SBU, where four polyhedrons around the central atoms are interconnected by sharing edges with each other. It is worth noting that four carboxylate groups display κ^1 and $(\kappa^2\text{-}\mu_2)$ binding fashions, respectively (Scheme S2, Mode III, Supporting Information). The Cd_4 SBUs are further bridged by six $dcpp^{4-}$ and two 2,2′-bipy to generate a 3D framework (Figure 3b) with 1D channels running along the *b* direction. The solvent-accessible volume and porosity are 1360.4 $Å^3$ and 20.3%, respectively, calculated by PLATON.[14] As each Cd_4 cluster links six $dcpp^{4-}$ and each $dcpp^{4-}$ connects three Cd_4 clusters, the whole skeleton could be viewed as a (3,6)-connected net with $(4^4{\cdot}6^2{\cdot}8^7{\cdot}10^2)(4^2{\cdot}6)$ topology (Figure 3c).

Crystal Structure of $\{[Cd_2(dcpp)(4,4'\text{-bipy})_{0.5}(H_2O)_3]\cdot H_2O\}_n$ (4). Complex **4** crystallizes in the monoclinic space group $P2_1/c$. Cd1 exhibits a distorted octahedral geometry that is completed with one O1 atom of one $dcpp^{4-}$, one O11 atom from one μ_2-OH_2, and two O atoms (O9, O10) of two terminal H_2O molecules at the equatorial plane, as well as another two carboxylate O atoms occupying the axial site. Cd2 is octahedrally coordinated and surrounded by four carboxylate O atoms (O1, O3, O4, O8), one μ_2-OH_2, and one N1 atom of one 4,4′-bipy (Cd−O/N = 2.200−2.458 Å) (Figure 4a). The four carboxylate groups adopt the (κ^1)-$(\kappa^1\text{-}\kappa^1)$-$(\kappa^1\text{-}\kappa^1)$-$(\mu_2)$-$\mu_6$ coordination fashion (Scheme S2, Mode IV, Supporting Information) to bridge three Cd1 and three Cd2. It is noted that two carboxylate groups in $(\kappa^1\text{-}\kappa^1)$ and μ_2 modes,

dx.doi.org/10.1021/cg401601d | *Cryst. Growth Des.* 2014, 14, 730−738

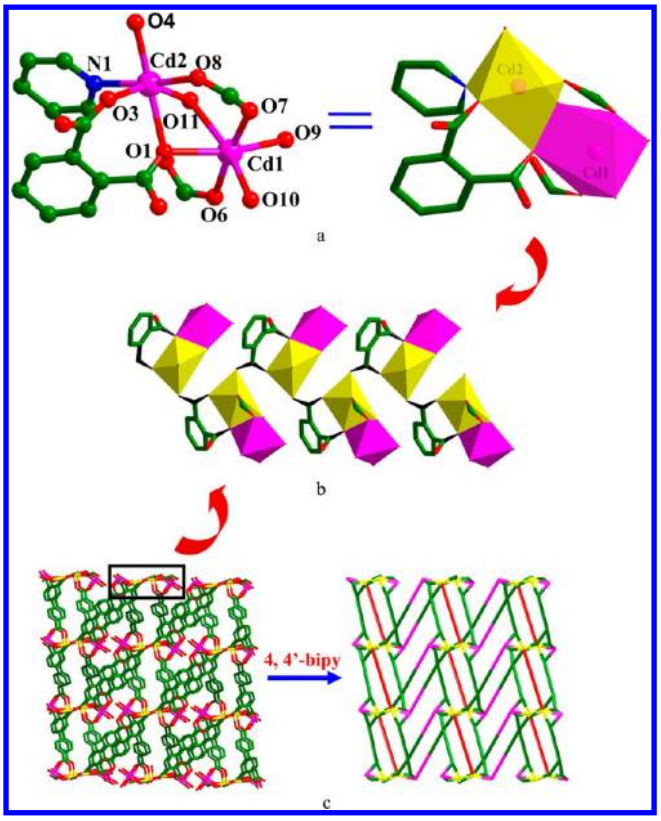

Figure 4. (a) Coordination environment around Cd^{II} in **4**. (b)The botryoid-like Cd cluster SBU. (c) The 3D network.

respectively, together with the μ_2-OH_2 bridge, link Cd1 and Cd2 to form an edge-sharing Cd_2 cluster in which the Cd1−Cd2 separation is 3.6622 Å. Interestingly, each Cd_2 unit is connected by the carboxylate groups in the (κ^1-κ^1) mode, yielding an infinite botryoid-like Cd cluster chain (Figure 4b) as the SBU. The distances between the Cd centers are Cd1−Cd1A = 9.8759 Å and Cd2−Cd2B = 4.9161 Å, respectively. To our best knowledge, MOFs constructed from such infinite Cd cluster chains as SBUs remain largely unexplored. The Cd cluster chains are connected with $dcpp^{4-}$, forming a 3D skeleton (Figure 4c left). Then the 4,4-bipy bind adjacent Cd1 ions to decorate the structure(Figure 4c, right).

Diverse Coordination Modes of H_4dcpp and Their Influences on the SBUs. As shown in Scheme S2 (Supporting Information), H_4dcpp are completely deprotonated and their coordination sites are fully occupied by Cd(II). Complexes **1**−**4** exhibit diverse structural features based on different SBUs. In complex **1**, the four carboxylate groups exhibit the uniform κ^2 coordination fashion (Mode I), and as a tetradentate ligand link Cd1 and Cd2 to produce 2D wavelike sheets. Adjacent sheets are then joined by the beb into a beautiful 3D structure. Because of the simple coordination fashion of H_4dcpp, there is no cluster-based second building unit in complex **1**. For complex **2**, in comparison with the coordination mode of **1**, the coordination modes of $dcpp^{4-}$ have some changes. Besides the simple κ^2 coordination fashion, the two carboxylate groups exhibit another two coordination modes (Mode II): one carboxylate group connects two Cd(II) (Cd1 and Cd2) by adopting the (κ^1-κ^1)-μ_2 fashion, and the other one adopts the (κ^2-μ_2) fashion to link two Cd(II) (Cd1 and Cd2). Then Cd1 is connected to adjacent Cd2 by two carboxylate groups to produce a corner-sharing Cd_2 unit where the Cd1···Cd2 separation is 3.9320 Å. The binuclear units are bridged with six $dcpp^{4-}$ to yield 2D puckered sheets, which are held together via the bmb to produce a 3D pillar-layered framework. As to complex **3**, the coordination mode of H_4dcpp is more complicated than that of complex **2**. Four carboxylate groups show κ^1 and (κ^2-μ_2) coordination fashions, respectively (Mode III). Cd1 and adjacent Cd2 are connected by two carboxylate groups, affording a Cd_2 cluster in which the Cd1···Cd2 separation is 3.724 Å. Two Cd_2 units are further connected by carboxylate groups, yielding an unusual Cd_4 cluster as the SBU. Then the Cd_4 clusters are linked by six $dcpp^{4-}$ to yield a porous skeleton. As to complex **4**, the $dcpp^{4-}$ adopts four coordination fashions, and its connecting modes (Mode IV) are more complicated than those of complex **3**. Different from the above coordination modes, the simple chelating mode (κ^2) does not exist in the H_4dcpp of complex **4**. Instead, the four carboxylate groups adopt the (κ^1)-(κ^1-κ^1)-(κ^1-κ^1)-(μ_2)-μ_6 fashion. Two carboxylate groups, together with the μ_2-OH_2 bridge, link Cd1 and Cd2 to form an edge-sharing binuclear Cd_2 unit. Interestingly, the binuclear Cd_2 units are further connected by the carboxylate groups, forming infinite botryoid-like Cd cluster chains that are connected with $dcpp^{4-}$ and produce a complicated 3D structure. Obviously, the constructions of SBUs in these complexes are seriously affected by the diverse coordination fashions of carboxylate groups of H_4dcpp. The more complicated the coordination modes are, the more diverse the structures become.

Influence of N Ligands on the Diverse Frameworks. As we know, N-donor ligands were commonly used as the auxiliary ligands to modify diverse structures for their strong coordination ability to transition-metal ions.[15] In **1**, there exist two types of beb, which exhibit an asymmetrical *cis*-conformation. Interestingly, along the *a* axis, two kinds of beb link adjacent Cd(II) to give rise to two types of meso-helical chains, respectively. In complex **2**, there are also two kinds of bmb, and they all show a symmetrical *trans*-conformation. The same structural feature for complexes **1** and **2** is that beb and bmb acting as bidentate bridges connect the 2D wavelike sheets constructed by carboxylate groups to form 3D pillar-layered frameworks, respectively. The widely used ligands 2,2′-bipy and 4,4′-bipy, although they make no contributions to the control of dimensionality of complexes **3** and **4**, have an important influence on constructing diverse structures with distinct SBUs. Complex **3** shows a porous 3D framework based on Cd_4 clusters, whereas complex **4** exhibits a three-dimensional structure with rare infinite botryoid-like Cd cluster chains as the SBU.

Photoluminescence Properties. Luminescence properties of complexes have attracted much interest for the potential applications as photoactive materials. We investigated the solid-state emission spectra of **1**−**4** and H_4dcpp at room temperature. As shown in Figure 5, H_4dcpp is a highly conjugated organic linker and shows an intense fluorescent emission at 427 nm (λ_{ex} = 315 nm), which is attributed to the n−π* transition. As we know, the auxiliary ligands beb and bmb display strong fluorescence emissions at 309 nm (λ_{ex} = 293 nm), and 310 nm (λ_{ex} = 294 nm), respectively.[18] Hence, the emissions of complex **1** (405 nm, λ_{ex} = 292 nm) and **2** (399 nm, λ_{ex} = 283 nm) stem from the intraligand transitions of H_4dcpp.[19] For complexes **3** and **4**, they also display similar, but weak, fluorescence emissions at 399 nm (λ_{ex} = 284 nm) and 402 nm (λ_{ex} = 284 nm), respectively. The emissions of **3** and **4** are also in accordance with those of the ligands (H_4dcpp, 2,2′-bipy,[20]

dx.doi.org/10.1021/cg401601d | Cryst. Growth Des. 2014, 14, 730−738

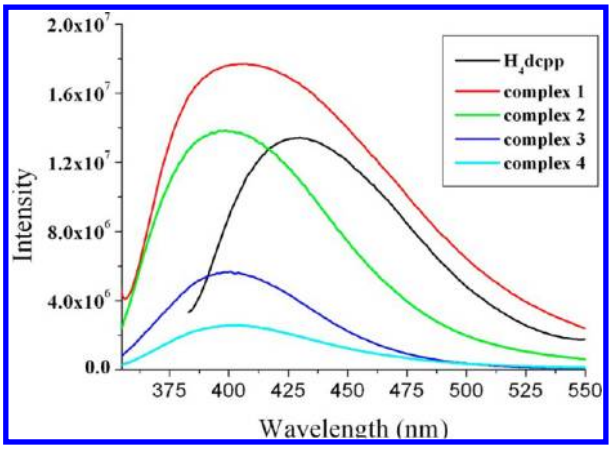

Figure 5. Emission spectra of H_4dcpp and complexes **1**−**4**.

and 4,4′-bipy[21]). The blue shift of emission bands for complexes **1**−**4** are due to the coordination interactions between the metals and the ligands.

Optical Band Gaps. Some cluster-based coordination complexes have potential application in semiconductive materials, [6] so we studied the band gaps E_g of complexes **1**−**4**. In a figure of K-M function versus energy, the band gap E_g is defined as the intersection point among the energy axis and line extrapolated of the linear portion.[16] The K-M function, $F = (1 - R)^2/2R$ (R is the reflectance of an infinitely thick layer at a given wavelength), can be converted from measured diffuse reflectance data. As shown in Figure S6 (Supporting Information), the E_g values for complexes **1**−**4** are 2.75, 2.59, 2.36, and 2.93 eV, respectively. The reflectance spectra show that there exist the optical band gap and semiconductive behaviors in complexes **1**−**4**, and these complexes can be employed as potential semiconductive materials (the E_g of a semiconductor is about 1−3 eV).[17]

Photocatalysis Property. To explore the efficacies of photocatalytic behavior of complexes **1**−**4**, the photocatalytic decomposition of 4-dimethylamino-azobenzene-4′-sulfonic acid sodium salt (methyl orange, MO) was investigated. Excitingly, complexes **1**−**4** exhibit good photocatalytic activities in the presence of H_2O_2 under high-pressure mercury lamp irradiation.

As the photocatalytic reaction continues, the absorption peak of MO significantly reduces (Figure 6). Moreover, the concentration changes in MO aqueous solution were plotted versus irradiation time (Figure 7). The degradation rate is 43% without any photocatalyst, and it increases to 97, 78, 85, and 67%, respectively, after irradiating complexes **1**−**4** for 100 min. The photocatalytic mechanism of the complexes is shown in Scheme S3 (Supporting Information). Under high-pressure mercury lamp irradiation, taking complex **1**, for example, its electrons (e^-) could be excited from the valence band (VB) to the conduction band (CB), leading to the equal amount of positive vacancies left in VB (holes, h+). By combining the electrons and O_2 absorbed on the photocatalyst surfaces, oxygen radicals ($\bullet O_2$) are generated initially, and then they transform into hydroxyl redicals ($\bullet$OH). Hydroxyl (OH^-)

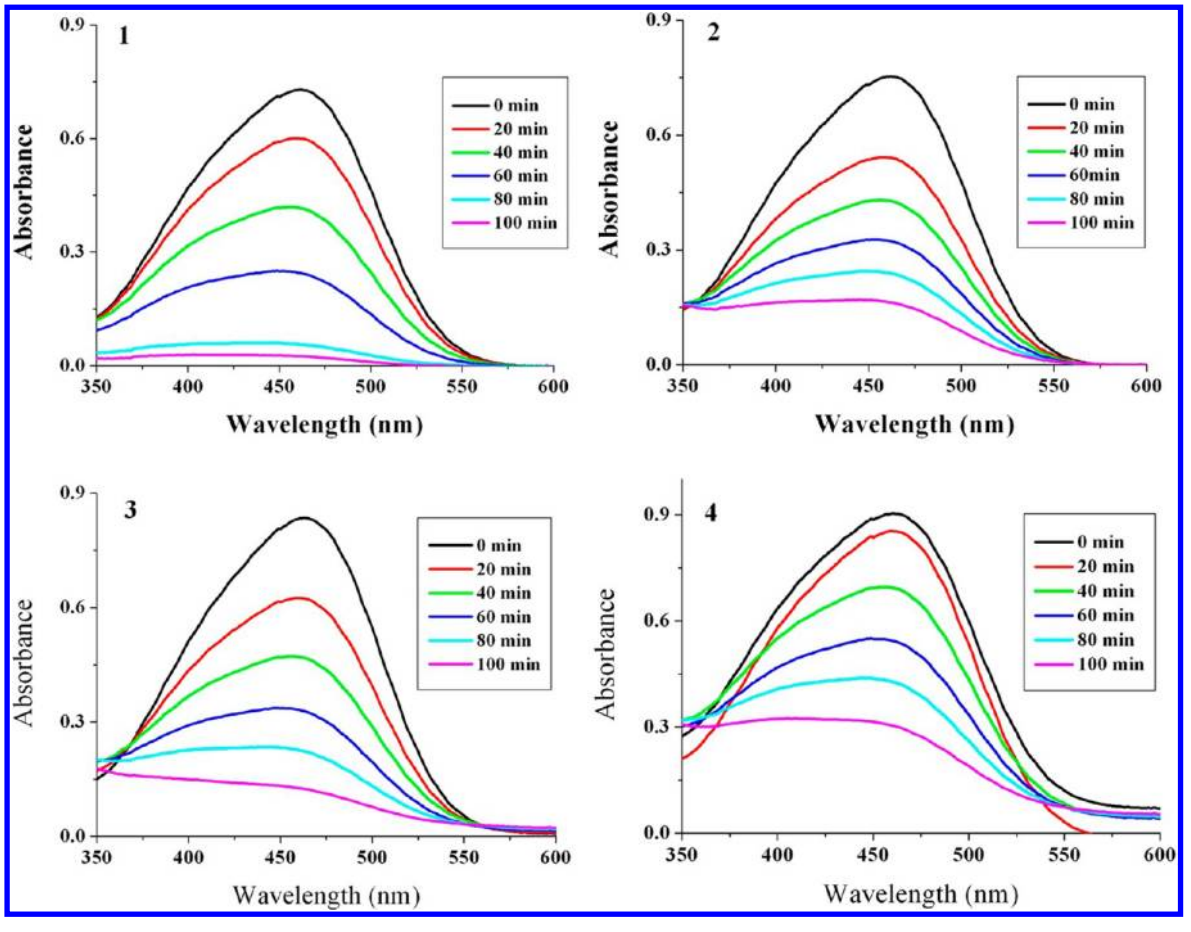

Figure 6. UV−vis absorption of MO at different time intervals under high-pressure Hg lamp irradiation with **1**−**4** as catalysts, respectively.

dx.doi.org/10.1021/cg401601d | Cryst. Growth Des. 2014, 14, 730−738

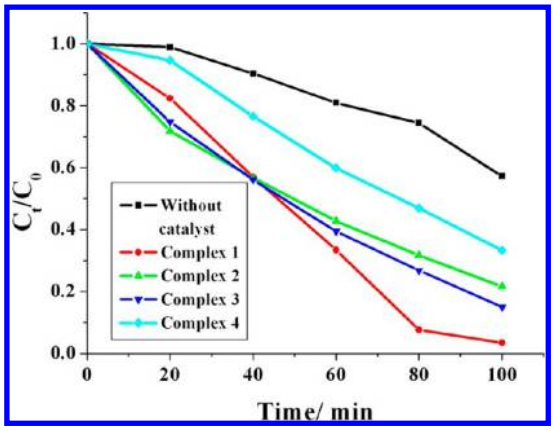

Figure 7. Concentration changes of MO at different time intervals under high-pressure Hg lamp irradiation without catalyst and with **1**–**4** as catalysts.

adsorbed on the surfaces of complex **1** interact with the hole (h^+) to generate hydroxyl radicals (•OH). Hydroxyl radicals (•OH) could effectively degenerate the methyl orange. It is worth noting that H_2O_2 is an indispensable member in the photocatalytic mechanism. H_2O_2 provides part of the O_2 and hydroxyl (OH^-) adsorbed on the surfaces of the complex and significantly accelerates the photocatalytic reaction.

According to the above photocatalytic mechanism, we know that the efficiency of the photocatalyst is a function of the balance between charge separation, interfacial electron transfer, and charge recombination. In general, a narrow band gap leads to the ease of the charge separation, so the photocatalytic decomposition rate of MO should follow the reverse order of band gaps of the complexes. As calculated, the band gaps of complexes **1**–**4** are 2.75, 2.59, 2.36, and 2.93 eV, respectively. The E_g of **2**–**4** follows the sequence **3** < **2** < **4**, and the reverse sequence of band gaps agrees with the decomposition rate of MO. However, for complex **1**, the band gap is not the narrowest among those of complexes **1**–**4**, and it exhibits extremely good photocatalytic activity. As functional carriers, the different SBUs may be responsible for the discrepancy in photocatalytic activities. It can be surmised that the noncluster-type SBUs facilitate the migration of excited electrons/holes and speed up the photocatalytic degradation process. In addition, we investigated the stabilities of complexes in the presence of H_2O_2 by measuring the powder PXRD patterns of the four complexes after photocatalytic reactions (Figure S7, Supporting Information). The PXRD patterns are consistent with those of the original ones, which confirm the stabilities of complexes **1**–**4** after the photocatalytic process. The photocatalytic research result indicates that complexes **1**–**4** are excellent candidates as photocatalysts in decomposing MO with the presence of H_2O_2 and may have possible application in decomposing other dyestuff.

CONCLUSIONS

Four cluster-based Cd/H_4dcpp/N-donor complexes as effective photocatalysts by adopting the strategy of constructing secondary building units have been synthesized. Our research demonstrates that coordination fashions of the polycarboxylate as well as adoption of the auxiliary N-donor ligands can effectively tune the kinds of SBUs and final structures. Complexes **1**–**4** display diverse structural features with the noncluster, dinuclear Cd cluster, the tetranuclear Cd cluster, and infinite botryoid-like Cd cluster chains as SBUs, respectively. Photocatalytic experiment results show that **1**–**4** are photocatalytically active for degrading MO under high-pressure mercury lamp irradiation, which are excellent candidates for decomposing other organic dyes.

ASSOCIATED CONTENT

Supporting Information

CIF files, bond angles and lengths, PXRD, TGAs, IR spectra, UV–vis absorption spectra, K-M functions vs energy, schematic representation of organic ligands, coordination fashions of H_4dcpp, and CCDC reference numbers 965277–965280. This information is available free of charge via the Internet at http://pubs.acs.org/.

AUTHOR INFORMATION

Corresponding Authors

*(J.D.) E-mail: jieding@zzu.edu.cn.

*(H.H.) E-mail: houhongw@zzu.edu.cn; Fax: 86-371-67761744.

Notes

The authors declare no competing financial interest.

ACKNOWLEDGMENTS

This research was supported by the National Natural Science Foundation (21371155) and the Research Fund for the Doctoral Program of Higher Education of China (20124101110002).

REFERENCES

(1) (a) Hoffmann, M. R.; Martin, S. T.; Choi, W.; Bahnemann, D. W. *Chem. Rev.* **1995**, *95*, 69–96. (b) Vandevivere, P. C.; Bianchi, R.; Verstraete, W. *J. Chem. Technol. Biotechnol.* **1998**, *72*, 289–302. (c) Waranusantigul, P.; Pokethitiyook, P.; Kruatrachue, M.; Upatham, E. S. *Environ. Pollut.* **2003**, *125*, 385–392.

(2) (a) Paul, A. K.; Madras, G.; Natarajan, S. *Phys. Chem. Chem. Phys.* **2009**, *11*, 11285–11296. (b) Zhuang, X.; Wan, Y.; Feng, C.; Shen, Y.; Zhao, D. *Chem. Mater.* **2009**, *21*, 706–716. (c) Yan, Y.; Zhang, M.; Gong, K.; Su, L.; Guo, Z.; Mao, L. *Chem. Mater.* **2005**, *17*, 3457–3463.

(3) (a) Ngah, W. S. W.; Hanafiah, M. A. K. M. *Bioresour. Technol.* **2008**, *99*, 3935–3948. (b) Lee, Y.; Zimmermann, S. G.; Kieu, A. T.; Gunten, U. V. *Environ. Sci. Technol.* **2009**, *43*, 3831–3838. (c) Sarasa, J.; Roche, M. P.; Ormad, M. P.; Gimeno, E.; Puig, A.; Ovelleiro, J. L. *Water Res.* **1998**, *32*, 2721–2727.

(4) (a) Legrini, O.; Oliveros, E.; Braun, A. M. *Chem. Rev.* **1993**, *93*, 671–698. (b) Mills, A.; Davies, R. H.; Worsley, D. *Chem. Soc. Rev.* **1993**, *22*, 417. (c) Tang, J.; Liu, Y.; Li, H.; Tan, Z.; Li, D. *Chem. Commun.* **2013**, *49*, 5498–5500. (d) Mahata, P.; Madras, G.; Natarajan, S. *J. Phys. Chem. B* **2006**, *110*, 13759–13768. (e) Wang, F.; Liu, Z. S.; Yang, H.; Tan, Y. X.; Zhang, J. *Angew. Chem., Int. Ed.* **2011**, *50*, 450–453. (f) Wen, L. L.; Wang, F.; Feng, J.; Lv, K. L.; Wang, C. G.; Li, D. F. *Cryst. Growth Des.* **2009**, *9*, 3581–3589. (g) Rajeshwar, K.; Tacconi, N. R.; Chenthamarakshan, C. R. *Chem. Mater.* **2001**, *13*, 2765–2782. (h) Wang, X. L.; Luan, J.; Sui, F. F.; Lin, H. Y.; Liu, G. C.; Xu, C. *Cryst. Growth Des.* **2013**, *13*, 3561–3576.

(5) (a) Kan, W. Q.; Liu, B.; Yang, J.; Liu, Y. Y.; Ma, J. F. *Cryst. Growth Des.* **2012**, *12*, 2288–2298. (b) Lin, H.; Maggard, P. A. *Inorg. Chem.* **2008**, *47*, 8044–8052. (c) Du, P.; Yang, Y.; Yang, J.; Liu, B. K.; Ma, J. F. *Dalton Trans.* **2013**, *42*, 1567–1580. (d) Cui, G. H.; He, C. H.; Jiao, C. H.; Geng, J. C.; Blatov, V. A. *CrystEngComm* **2012**, *14*, 4210–4216. (e) Sha, J. Q.; Sun, J. W.; Li, M. T.; Wang, C.; Li, G. M.; Yan, P. F.; Sun, L. J. *Dalton Trans.* **2013**, *42*, 1667–1677. (f) Liao, Z. L.; Li, G. D.; Bi, M. H.; Chen, J. S. *Inorg. Chem.* **2008**, *47*, 4844–4853.

(6) (a) Tranchemontagne, D. J.; Mendoza-Cortés, J. L.; O'Keeffe, M.; Yaghi, O. M. *Chem. Soc. Rev.* **2009**, *38*, 1257–1283. (b) Basu, T.;

Sparkes, H. A.; Bhunia, M. K.; Mondal, R. *Cryst. Growth Des.* **2009**, *9*, 3488−3496. (c) Chun, H.; Jung, H. *Inorg. Chem.* **2009**, *48*, 417−419. (d) Yi, F. Y.; Sun, Z. M. *Cryst. Growth Des.* **2012**, *12*, 5693−5700. (e) Cui, J.; Li, Y.; Guo, Z.; Zheng, H. *Chem. Commun.* **2013**, *49*, 555−557.

(7) (a) Das, M. C.; Xiang, S.; Zhang, Z.; Chen, B. *Angew. Chem., Int. Ed.* **2011**, *50*, 10510−10520. (b) Li, J. R.; Sculley, J.; Zhou, H. C. *Chem. Rev.* **2012**, *112*, 869−932. (c) Farrusseng, D.; Aguado, S.; Pinel, C. *Angew. Chem., Int. Ed.* **2009**, *48*, 7502−7513. (d) Ford, P. C.; Cariati, E.; Bourassa, J. *Chem. Rev.* **1999**, *99*, 3625−3647.

(8) (a) Xiang, S.; Zhou, W.; Gallegos, J. M.; Liu, Y.; Chen, B. *J. Am. Chem. Soc.* **2009**, *131*, 12415−12419. (b) Rosi, N. L.; Kim, J.; Eddaoudi, M.; Chen, B.; O'Keeffe, M.; Yaghi, O. M. *J. Am. Chem. Soc.* **2005**, *127*, 1504−1518. (c) Llewellyn, P. L.; Bourrelly, S.; Serre, C.; Vimont, A.; Datuti, M.; Hamon, L.; Weireld, G. D.; Chang, J. S.; Hong, D. Y.; Hwang, Y. K.; Jhung, S. H.; Férey, G. *Langmuir* **2008**, *24*, 7245−7250.

(9) (a) Han, S. D.; Song, W. C.; Zhao, J. P.; Yang, Q.; Liu, S. J.; Li, Y.; Bu, X. H. *Chem. Commun.* **2013**, *49*, 871−873. (b) Yao, R. X.; Xu, X.; Zhang, X. M. *Chem. Mater.* **2012**, *24*, 303−310. (c) Cheng, X. N.; Zhang, W. X.; Lin, Y. Y.; Zheng, Y. Z.; Chen, X. M. *Adv. Mater.* **2007**, *19*, 1494−1498.

(10) (a) Xiao, Y.; Cui, Y.; Zheng, Q.; Xiang, S.; Qian, G.; Chen, B. *Chem. Commun.* **2010**, *46*, 5503−5505. (b) Guo, X.; Zhu, G.; Sun, F.; Li, Z.; Zhao, X.; Li, X.; Wang, H.; Qiu, S. *Inorg. Chem.* **2006**, *45*, 2581−2587. (c) He, J.; Yu, J.; Zhang, Y.; Pan, Q.; Xu, R. *Inorg. Chem.* **2005**, *44*, 9279−9282.

(11) (a) Park, T. H.; Hickman, A. J.; Koh, K.; Martin, S.; Wong-Foy, A. G.; Sanford, M. S.; Matzger, A. J. *J. Am. Chem. Soc.* **2011**, *133*, 20138−20141. (b) Horike, S.; Dincă, M.; Tamaki, K.; Long, J. R. *J. Am. Chem. Soc.* **2008**, *130*, 5854−5855. (c) Jeong, K. S.; Go, Y. B.; Shin, S. M.; Lee, S. J.; Kim, J.; Yaghi, O. M.; Jeong, N. *Chem. Sci.* **2011**, *2*, 877−882. (d) Vermoortele, F.; Vandichel, M.; Voorde, B. V.; Ameloot, R.; Waroquier, M.; Speybroeck, V. V.; Vos, D. E. D. *Angew. Chem., Int. Ed.* **2012**, *51*, 4887−4890.

(12) (a) Cao, J.; Gao, Y.; Wang, Y.; Du, C.; Liu, Z. *Chem. Commun.* **2013**, *49*, 6897−6899. (b) Pang, L. Y.; Liu, P.; Zhang, C. P.; Chen, X.; Chen, B.; Wang, Y. Y.; Shi, Q. Z. *Inorg. Chim. Acta* **2013**, *403*, 43−52.

(13) (a) Sheldrick, G. M. *SHELXS 97: Program for the Solution of Crystal Structures*; University of Göttingen: Göttingen, Germany, 1997. (b) Sheldrick, G. M. *SHELXS 97: Program for the Refinement of Crystal Structures*; University of Göttingen: Göttingen, Germany, 1997.

(14) Spek, A. L. *J. Appl. Crystallogr.* **2003**, *36*, 7.

(15) (a) Bisht, K. K.; Suresh, E. *Inorg. Chem.* **2012**, *51*, 9577−9579. (b) Demadis, K. D.; Panera, A.; Anagnostou, Z.; Varouhas, D.; Kirillov, A. M.; Císařová, I. *Cryst. Growth Des.* **2013**, *13*, 4480−4489. (c) Zhao, W.; Han, J.; Tian, G.; Zhao, X. Li. *CrystEngComm* **2013**, *15*, 7522−7530. (d) Zhou, K.; Jiang, F. L.; Chen, L.; Wu, M. Y.; Zhang, S. Q.; Ma, J.; Hong, M. C. *Chem. Commun.* **2012**, *48*, 12168−12170. (e) Hu, F. L.; Wu, W.; Liang, P.; Gu, Y. Q.; Zhu, L. G.; Wei, H.; Lang, J. P. *Cryst. Growth Des.* **2013**, *13*, 5050−5061.

(16) (a) Gong, Y.; Hao, Z.; Sun, J. L.; Shi, H. F.; Jiang, P. G.; Lin, J. H. *Dalton Trans.* **2013**, *42*, 13241−13250. (b) Zhang, L.; Wei, Y.; Wang, C.; Guo, H.; Wang, P. *J. Solid State Chem.* **2004**, *177*, 3433−3438.

(17) (a) Silva, C. G.; Corma, A.; García, H. *J. Mater. Chem.* **2010**, *20*, 3141−3156. (b) Tachikawa, T.; Choi, J. R.; Fujitsuka, M.; Majima, T. *J. Phys. Chem. C* **2008**, *112*, 14090−14101. (c) Alvaro, M.; Carbonell, E.; Ferrer, B.; Xamena, F. X. L.; Garcia, H. *Chem.—Eur. J.* **2007**, *13*, 5106.

(18) Xu, C.; Guo, Q.; Wang, X.; Hou, H.; Fan, Y. *Cryst. Growth Des.* **2011**, *11*, 1869−1879.

(19) (a) Xiao, D. R.; Li, Y. G.; Wang, E. B.; Fan, L. L.; An, H. Y.; Su, Z. M.; Xu, L. *Inorg. Chem.* **2007**, *46*, 4158−4166. (b) Zhang, J.; Li, Z. J.; Kang, Y.; Cheng, J. K.; Yao, Y. G. *Inorg. Chem.* **2004**, *43*, 8085−8091.

(20) Gong, Y.; Jiang, P. G.; Li, J.; Wu, T.; Lin, J. H. *Cryst. Growth Des.* **2013**, *13*, 1059−1066.

(21) Zhang, S. Q.; Jiang, F. L.; Wu, M. Y.; Ma, J.; Bu, Y.; Hong, M. C. *Cryst. Growth Des.* **2012**, *12*, 1452−1463.